

## In-Plane Lattice Reconstruction of Cu(100)

S. Müller, A. Kinne, M. Kottcke, R. Metzler, P. Bayer, L. Hammer, and K. Heinz

*Lehrstuhl für Festkörperphysik, Universität Erlangen-Nürnberg, Staudtstrasse 7, D-91058 Erlangen, Germany*  
(Received 6 July 1995)

A new structural analysis of the clean Cu(100) surface by low energy electron diffraction yields a surprising in-plane lattice contraction of about 1% compared to the bulk lattice parameter, i.e., a surface reconstruction following the tensile stress in the surface. This sheds new light on the epitaxial growth of other metals on Cu(100). Additionally, we report on a similar contraction determined for the metastable  $1 \times 1$  phase of the (100) surface of platinum indicating that in-plane lattice reconstruction might be a more general feature than believed.

PACS numbers: 68.35.Bs, 61.14.Hg, 61.66.Bi, 68.10.Cr

Structure analyses of unreconstructed surfaces of clean crystals usually do not aim at the determination of the surface parallel (or in-plane) lattice parameter  $a_p$ . By symmetry arguments the latter is believed to be the same as in bulk layers; otherwise structural defects must be introduced when the surface is created. On the other hand, each surface exhibits a tensile stress [1–9] favoring the formation of more densely packed layers. In fact, a few clean surfaces as the stable (100) surfaces of Au, Pt, and Ir and the (111) surfaces of Pt and Au are known to reconstruct in this sense. As these examples are considered rather exceptional, we show in the present Letter that the feature of in-plane reconstruction might be more general (though not universal): Cu(100), when prepared in a conventional way, reconstructs by a 1% contraction of the in-plane lattice parameter. The same holds for the metastable  $1 \times 1$  phase of Pt(100) possibly being a precursor to the full hexagonal reconstruction.

Our reinvestigation of Cu(100) was triggered by work on the heteroepitaxial growth of metals on copper. For Fe/Cu(100)  $a_p(\text{Fe}) = 2.52 \text{ \AA}$  was found [10–13] contrasting  $a_p(\text{Cu}) = 2.55 \text{ \AA}$  for bulk copper. In fact, nonpseudomorphic growth of Fe was concluded [10,11]. For the system Ni/Cu(100) a value  $a_p(\text{Ni}) = 2.53 \text{ \AA}$  was determined [14,15]. These results suggest that it might be a reduced in-plane lattice parameter of Cu(100) that determines the lattice of the epitaxial films. We applied low energy electron diffraction (LEED) for the determination of  $a_p$ . In view of the small contraction we had to accept that—different from the surfaces of Pt, Ir, and Au—no superstructure spots show up when a conventional LEED optics is used. So, detection of the reconstruction can only come by the measurement of accurate data and their careful dynamical analysis.

The copper crystal (5N purity,  $\pm 0.5^\circ$  orientation accuracy) was mechanically polished (1  $\mu\text{m}$  minimum grain size). *In situ* cleaning by Ar ion bombardment (600 V, 1  $\mu\text{A}/\text{cm}^2$ , 800 K) and annealing (1000 K) yielded a surface with impurities like O, C, and S below the Auger detection limit ( $\leq 3\%$ ) and a low background diffraction pattern. Intensities were taken at 90 K to reduce thermal

diffuse scattering. A video based data acquisition system was used [16–18] whose speed made residual gas adsorption negligible. Measurement of five beams symmetrically inequivalent at normal incidence produced a database with total width  $\Delta E = 1600 \text{ eV}$ . Adjustment of normal incidence was made by the comparison of symmetrically equivalent beams and judged to be satisfying when the Pendry  $R$  factor  $R_p$  [19] was below 0.04. Residual misalignment was corrected by a final averaging of equivalent spectra. The data were reproducible within a level  $R_p < 0.02$ .

Intensities were analyzed full dynamically using standard programs [20,21]. The layer diffraction matrices were computed by matrix inversion, and the layers were stacked using the layer doubling scheme. A maximum of 14 phase shifts calculated relativistically with eventual spin averaging were used. They were corrected for thermal vibrations using the bulk Debye temperature of copper ( $\Theta_b = 443 \text{ K}$ ) for subsurface layers and a value  $\Theta_s$  to be fitted for the top surface layer. For the best fit search the parameter space was scanned on a dense grid. This was made up by the first six interlayer distances  $d_{ik}$ , the bulk distance  $d_b$  for deeper layers, and additionally  $a_p$ , all of them varied independently in steps of 1/100  $\text{\AA}$ . By design of LEED programs the same value of  $a_p$  had to be assumed for all layers. As usual, electron attenuation was described by an optical potential. Together with the real part of the inner potential it was determined in the course of the fit [20,21]. For the quantitative comparison of experimental and calculated data predominantly the Pendry  $R$  factor was used. Occasionally, also their relative mean square deviation  $R_2$  was applied.

The best fit results with minimum  $R$  factors  $R_p = 0.085$  and  $R_2 = 0.018$ . Such values belong to the very best reported for LEED analyses. The variation of  $R_p$  with  $a_p$  with all other parameters optimized to produce the global best fit is displayed in Fig. 1. There is a clear minimum at  $a_p = 2.53 \text{ \AA}$ . The strong variation may surprise one in view of the fact that for normal incidence data there is usually only a little sensitivity with respect to surface parallel

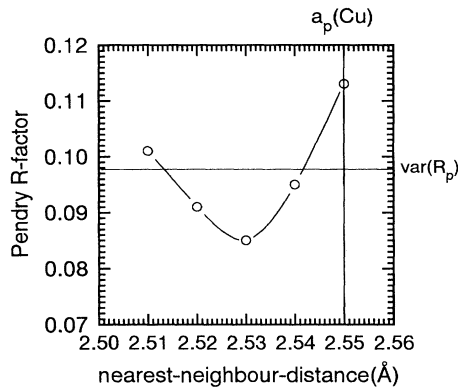


FIG. 1. Variation of the best-fit Pendry  $R$  factor with varying in-plane lattice parameter  $a_p$ . The vertical line corresponds to the bulk value  $a_p = 2.55$  Å, and the horizontal line indicates the level of the  $R$ -factor variance above the minimum  $R$  factor.

parameters as  $a_p$ . However, this is only true for considerably higher  $R$ -factor levels. For that displayed in Fig. 1 ( $R_p < 0.12$ ) the sensitivity comes back because theoretical and experimental data are close enough to make the small changes introduced by the variation of  $a_p$  detectable. The corresponding best fit values for the other parameters are  $d_{12} = 1.765 \pm 0.005$  Å,  $d_{23} = 1.805 \pm 0.010$  Å,  $d_{34} = 1.80 \pm 0.01$  Å,  $d_{45} = 1.80 \pm 0.02$  Å,  $d_{56} = 1.80 \pm 0.03$  Å,  $d_{67} = 1.79 \pm 0.04$  Å,  $d_b = 1.79 \pm 0.07$  Å, and  $\Theta_s = 235_{-20}^{+60}$  K. For vertical distances the error limits increase with increasing depth because of electron attenuation. They derive from the variance of the Pendry  $R$  factor, i.e., by assuming *statistical* errors only [19]. The variance is given by  $\text{var}(R_p) = R_p \min(8V_{0i}/\Delta E)^{1/2}$ , where  $\Delta E$  is the energy width of the database ( $\Delta E = 1600$  eV). All structural models with  $R_p \leq R_{p \min} + \text{var}(R_p)$  are within the limits of error. With  $\text{var}(R_p) = 0.013$  the  $R$ -factor limit is  $R_p = 0.098$  represented by the horizontal line in Fig. 1. As a consequence, the error limits for  $a_p$  can be written as  $a_p = 2.53 \pm 0.01$  Å. So, the bulk value of 2.55 Å can be ruled out; this is most likely since this kind of error estimation is experienced to be rather conservative. Experimental and best fit spectra compare very well also visually as demonstrated in Fig. 2 for two beams.

Though the contraction is outside the limits of statistical errors, possible *systematic* errors in the LEED structure determination should be discussed before taking the result seriously. Therefore, as a general test we applied the same type of analysis to another clean metal surface. We chose the (100) surface of the random alloy  $\text{Mo}_{75}\text{Re}_{25}$  because for this an earlier investigation [22] had produced an  $R$  factor sufficiently low for the determination of  $a_p$ . The analysis yields  $a_p = 3.125 \pm 0.01$  Å in perfect agreement with the bulk value,  $a_p = 3.127$  Å [23]. The minimum  $R$  factors are  $R_p = 0.117$  and  $R_2 = 0.030$ . The result proves that our procedure of structure determi-

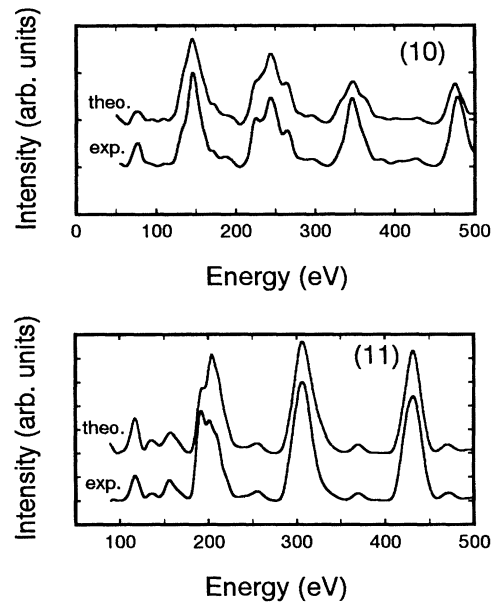


FIG. 2. Comparison of experimental and calculated best-fit spectra for some selected beams.

nation has no built-in features that automatically yield a reduced in-plane lattice constant.

Therefore, the next test must apply to possible errors applying to Cu(100) only. For the calculation of intensities the material specific input is the set of phase shifts used. Within the muffin-tin approximation of the scattering potential the muffin-tin radius  $r_{\text{mft}}$  is the most important parameter, and we therefore produced different sets of phase shifts for varying values of  $r_{\text{mft}}$ . For each set the structure was optimized separately. Figure 3 displays the corresponding variation of  $R_p$  for two fixed values of  $a_p$ , i.e., the critical values  $a_p = 2.53$  and 2.55 Å. For the best fit value,  $a_p = 2.53$  Å, the  $R$  factor is rather insensitive with respect to  $r_{\text{mft}}$ , at least in the relevant range of 2.40–2.55 Å. For  $a_p = 2.55$  Å,  $R_p$  varies strongly and meets the level obtained for  $a_p = 2.53$  Å only at rather unphysical values of  $r_{\text{mft}}$ . It never reaches the minimum

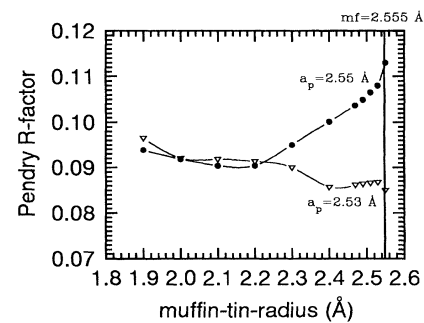


FIG. 3. Variation of the Pendry  $R$  factor with varying muffin-tin radius for two fixed values of  $a_p$ .

value  $R_{p \min} = 0.085$ . Consequently, the lattice contraction derived is unlikely to be due to a wrong choice of  $r_{\text{mft}}$ .

Another assumption made in the calculations is the real part of the inner potential  $V_{0r}$  being constant. Though  $V_{0r}$  is known to vary with energy [24], it is common experience that using a constant average does not lead to incorrect structural parameters. Only an increased level of the minimum  $R$  factor results. The very low level reached for Cu(100) means that all peaks are almost in the correct positions. Consequently, the question is whether a deviation from the correct value of  $V_{0r}$  can be compensated by a deviation from the correct value of  $a_p$ . However, in the kinematic approximation [25] a wrong choice of  $a_p$  induces only an energy independent shift of  $V_{0r}$  and, additionally, the latter is different for different beams. As this was not observed in our investigation, an ill defined value of  $V_{0r}$  should not cause the observed contraction.

Finally, we checked for experimental errors caused by an imperfect sample. Deviations from an ideal flat surface as assumed in the calculation may cause small errors. The miscut of our sample being  $0.5^\circ$  at maximum causes steps with an average terrace width of slightly above 200 Å. This is larger than the transfer width of our electron optics and so is very unlikely to influence intensities to a measurable extent. However, it is well known that a macroscopic flat surface can exhibit some mosaic structure with domains misoriented with respect to each other by a certain angle. This leads to a broadening of diffraction spots and—for the intensities from a single domain—breaks the degeneracy of spots symmetrically equivalent at exact normal incidence. From the spot widths observed we deduce that the deviations from the macroscopic surface normal are smaller than  $0.5^\circ$ . For such small values the influence of the mosaic structure should largely cancel both by the presence of many + and – oriented domains as well as by the averaging of symmetrically equivalent beams. For a quantitative test we calculated intensities for a misalignment of  $0.5^\circ$  off normal incidence, so that the 10 and  $\bar{1}0$  beam spectra become different. Their mutual  $R$  factor is  $R_p = 0.07$ . However, averaging of the 10 and  $\bar{1}0$  spectra, as routinely carried out for the experimental data, yields a spectrum that compares to that calculated for exact normal incidence by an  $R$  factor as low as  $R_p = 0.004$ . Therefore, a mosaic structure simulating the in-plane contraction can also be ruled out.

Consequently, our result of a reconstructed Cu(100) surface must be taken as a fact. With the same value of  $a_p$  assumed for the different layers, the contraction determined reflects an average value over layers covered by the electron penetration depth. This means that in principle the contraction in the very surface layer could be even higher than 1% with a layer-by-layer accommodation to the bulk value. On a first glance this seems to be rather unlikely in view of the lattice

parameters of 2.52–2.53 Å determined for epitaxial Fe and Ni films on Cu(100). However, adsorption may reduce surface stress, so that a higher top layer contraction could be partly released through film deposition. In any case, our result shows that the epitaxial growth of Fe and Ni on Cu(100) is pseudomorphic.

A small contraction requires the formation of defects as grain boundaries. Also, the presence or formation of steps may help to accommodate the surface to the bulk lattice. For a 1% contraction defects should appear every 100 lattice constants (250 Å) on an average. This is again considerably larger than the transfer width of a conventional LEED optics ( $\sim 100$  Å). So, the usual LEED experiment cannot be expected to be sensitive to defects of the density mentioned. We should also point out that by conventional procedures applied for the preparation of copper crystals as described above, such defects are very likely to be induced. However, if removal of defects by sophisticated sample preparation results in a flat surface, there should be no surface contraction as obvious from symmetry arguments.

The in-plane reconstruction detected for Cu(100) is not very surprising if one considers earlier investigations dealing with its surface stress. So, the Rayleigh phonon dispersion found could be explained by either a modified force constant between the first and second layers or a considerable surface stress with “a tendency of the surface layer to contract” [26]. Calculations of surface stress using embedded atom method potentials yielded a value only about a factor of 2 smaller than that obtained for the Pt(100)-(1 × 1) surface [27]. This surface reconstructs to Pt(100)-(5 × 20) forming a hexagonally close packed top layer. By additional application of stability criteria it was therefore suggested that there may be significant driving force for such a reconstruction also for Cu(100) and that some kinetic barrier inhibits the reconstruction process [27]. More recently, *ab initio* calculations for Pt(100) using density functional theory yielded a large surface stress of 2.69 eV/(unit cell area) [28]. Moreover, it was found that a large surface stress is not sufficient to drive the reconstruction process of the top layer. Only when the bonding to the substrate is weak enough to keep the energy cost for the developing surface-substrate mismatch smaller than the energy gain by release of surface stress, will the reconstruction take place [28].

As the Pt(100) surface can be prepared in a metastable 1 × 1 phase that reconstructs to Pt(100)-(5 × 20) in a thermally activated process [29], it would be interesting to know which lattice parameter applies for the 1 × 1 phase. Following the above arguments one would expect that a continuous contraction should take place until the energy gain is balanced by the simultaneously increasing cost of mismatch energy. The latter is determined by the size of domains in which the lattice contracts. The domains are separated by defects, and the energy for their creation adds to the total energy cost.

We therefore eventually carried out a LEED structure determination for Pt(100)-(1 × 1) in essentially the same way as for Cu(100). The preparation of the 1 × 1 phase was described earlier [29]. The result for the in-plane lattice parameter yields the value  $a_p = 2.754 \pm 0.02$  Å, which compared to the bulk value (2.774 Å) corresponds again to a 1% contraction. The minimum average  $R$  factor is  $R_p = 0.179$ . Because of their larger in-plane momentum transfer higher order beams react more significantly to the contraction than low index beams. So, the  $R$  factor for, e.g., the 30 beam reduces from  $R_p = 0.22$  to 0.09.

Though the surface stress for Pt(100) is likely to be larger by a factor of 2 than for Cu(100), the contraction has about the same relative magnitude. This is not contradictory because, as pointed out above, the amount of contraction is controlled by a delicate balance between energy gain and cost caused by the stress release and mismatch, respectively. The latter should depend on the size of domains and the defects created between them. In contrast to copper, for platinum there is a global minimum of the total energy only when the top layer contracts to a hexagonal arrangement. In this sense the contraction saving quadratic symmetry may be interpreted as a precursor to the full reconstruction developing with thermal activation. [We expect the same qualitative behavior for Au(100) and Ir(100), which also can be prepared in metastable 1 × 1 phases [30,31].] For  $\text{Mo}_{0.75}\text{Re}_{0.25}$ (100) the first to second layer interaction obviously is large enough or the surface is so perfect that any contraction is inhibited. In general, however, surface in-plane lattice contraction should be more a rule than an exception.

We gratefully acknowledge financial support through the Deutsche Forschungsgemeinschaft (DFG).

- 
- [1] W. Gibbs, *Collected Works* (Longmans and Green, New York, 1928), Vol. 1.
  - [2] C. Herring, in *The Physics of Powder Metallurgy*, edited by W. E. Kingston (McGraw-Hill, New York, 1951).
  - [3] C. Herring, in *Structure and Properties of Solid Surfaces*, edited by R. Gomer and C. S. Smith (University of Chicago Press, Chicago, 1953).

- [4] J. S. Vermaak, C. W. Mays, and D. Kuhlmann-Wilsdorf, *Surf. Sci.* **12**, 128 (1968).
- [5] R. J. Needs, *Phys. Rev. Lett.* **58**, 53 (1987).
- [6] M. C. Payne, N. Roberts, R. J. Needs, and J. D. Joannopoulos, *Surf. Sci.* **211/212**, 1 (1989).
- [7] R. J. Needs and M. J. Godfrey, *Phys. Scr.* **T19**, 319 (1987).
- [8] R. C. Cammarata, *Surf. Sci.* **279**, 341 (1992).
- [9] H. Ibach, *J. Vac. Sci. Technol. A* **12**, 2240 (1994).
- [10] P. Bayer, S. Müller, P. Schmailzl, and K. Heinz, *Phys. Rev. B* **48**, 17 611 (1993).
- [11] S. Müller, P. Bayer, A. Kinne, P. Schmailzl, and K. Heinz, *Surf. Sci.* **322**, 21 (1995).
- [12] J. V. Barth and D. E. Fowler, *Phys. Rev. B* (to be published).
- [13] H. Magnan, D. Chanderis, B. Vilette, O. Hechmann, and J. Lecante, *Phys. Rev. Lett.* **67**, 859 (1991).
- [14] B. Schulz, S. Müller, G. Kostka, M. Farle, K. Heinz, and K. Baberschke, *Verhandl. DPG (VI)* **30**, 1486 (1995).
- [15] S. Müller, B. Schulz, G. Kostka, M. Farle, K. Heinz, and K. Baberschke (to be published).
- [16] K. Müller and K. Heinz, in *The Structure of Surfaces*, Springer Series in Surface Sciences Vol. 2 (Springer, Berlin, 1985), p. 105.
- [17] K. Heinz, *Prog. Surf. Sci.* **27**, 239 (1988).
- [18] K. Heinz, *Rep. Prog. Phys.* **58**, 637 (1995).
- [19] J. B. Pendry, *J. Phys. C* **13**, 937 (1980).
- [20] J. B. Pendry, *Low Energy Electron Diffraction* (Academic Press, London, 1974).
- [21] M. A. Van Hove and S. Y. Tong, *Surface Crystallography by LEED* (Springer, Berlin, 1979).
- [22] R. Döll, M. Kottcke, K. Heinz, L. Hammer, K. Müller, and D. M. Zehner, *Surf. Sci.* **307-309**, 434 (1994).
- [23] G. C. Wang, D. M. Zehner, and H. C. Eaton, *Mater. Res. Soc. Symp. Proc.* **87**, 29 (1987).
- [24] J. Neve, P. Westrin, and J. Rundgren, *J. Phys. C* **16**, 1291 (1983).
- [25] M. A. Van Hove, W. H. Weinberg, and C.-M. Chan, *Low-Energy Electron Diffraction* (Springer, Berlin, 1986).
- [26] M. Wuttig, R. Franchy, and H. Ibach, *Z. Phys. B* **65**, 71 (1986).
- [27] R. C. Cammarata, *Surf. Sci.* **279**, 341 (1992).
- [28] V. Fiorentini, M. Methfessel, and M. Scheffler, *Phys. Rev. Lett.* **71**, 1051 (1993).
- [29] K. Heinz, E. Lang, K. Strauss, and K. Müller, *Surf. Sci.* **120**, L401 (1982).
- [30] J. F. Wendelken and D. M. Zehner, *Surf. Sci.* **71**, 178 (1978).
- [31] J. Küppers and H. Michel, *Appl. Surf. Sci.* **3**, 179 (1979).